JOURNAL OF CATALYSIS 133, 370–382 (1992)

Hydrogen Effects on Nickel-Catalyzed Vapor-Phase Methanol Carbonylation

K. FUJIMOTO,*,[1] S. BISCHOFF,*,† K. OMATA,* AND H. YAGITA*

*Department of Synthetic Chemistry, Faculty of Engineering, University of Tokyo, Hongo, Bunkyo-ku, Tokyo 113, Japan; and †Department of C_1-Chemistry, Central Institute of Organic Chemistry, Rudower Chaussee 5, 0-1199 Berlin-Adlershof, Germany

Received October 17, 1990; revised March 22, 1991

The influence of hydrogen on the reaction orders of CO and methanol, with respect to the formation of acyl compounds, methane, and dimethyl ether, was investigated. Although hydrogen-promoted methane formation, experiments with deuterium and methanol-d_1 (MeOD) clarified that the hydrogen of the methanol hydroxyl group is the exclusive hydrogen source of the CH_4 formation and that this reaction occurs at nickel centers, which are also involved in the acyl compound formation. Temperature-programmed reaction (TPR) and X-ray diffraction (XRD) experiments suggested that the hydrogen effect is caused by changes in the number of active sites and that neither methanol carbonylation nor methane formation proceeds at the larger nickel[0] crystallites detectable by XRD. Furthermore, it has been demonstrated that under certain reaction conditions, hydrogen can induce a remarkable deactivation of the catalyst by promoting nickel aggregation. A mechanism that accounts for the hydrogen effects has been postulated.

INTRODUCTION

The vapor-phase carbonylation of methanol (MeOH) (Eq. (1)), catalyzed by Ni on activated carbon (Ni/A.C.) in the presence of methyl iodide (MeI), is considered to proceed via the oxidative addition of methyl iodide to Ni[0] species followed by CO insertion and the reductive methanolysis of Ni–acyl complexes. The first step proceeds rather quickly, while the following steps are known to determine the rate (*1*):

$$CH_3OH + CO \xrightarrow{\text{Ni/A.C., } CH_3I} \begin{cases} CH_3COOH,\ CH_3COOCH_3 + H_2O \\ CH_3OCH_3,\ CH_4,\ CO_2 \quad \text{(by-products)}. \end{cases} \tag{1}$$

Hydrogen has been reported as an effective promoter for methanol carbonylation both in the liquid phase (*2*) and in the vapor phase (*3–5*). The increased carbonylation activity, resulting in enhanced carbonylation of dimethyl ether (DME) to methyl acetate (AcOMe), has been discussed as the reason for the decreasing DME yields (*3*). However, the suppressed CO_2 and enhanced CH_4 formation in the presence of hydrogen has remained unclarified. The higher carbonylation activity in the presence of H_2 has been suggested to result from an increase in the number of active Ni sites (*3*). It has also been reported that in the presence of H_2 the reaction orders of MeOH and MeI with respect to acyl compound formation decreased or increased, respectively (*4*). The reaction orders for the formation of the by-products have not been determined.

Interestingly, the replacement of hydrogen by deuterium afforded only very small amounts of deuterated products (*4*), indicating that hydrogen does not directly react at

[1] To whom correspondence should be addressed.

0021-9517/92 $3.00

the active centers. This is also supported by the fact that, in the presence of hydrogen, hydrocarbonylation products such as acetaldehyde or its methyl acetals, have not been detected.

The undesired CH_4 formation has been supposed to result from the hydrogenolysis of Me–Ni–I species, although the hydrogen source was not clearly assigned (*4*). Additional studies on the influence of temperature and nickel loading should provide more detailed information on hydrogen effects.

This work is aimed at the clarification of the above-mentioned problems and at a generally deeper understanding of the complex mechanism of the carbonylation reaction.

EXPERIMENTAL

The catalytic experiments were conducted in a previously described stainless-steel fixed-bed reactor (*1*), using activated carbon-supported Ni catalysts (Ni/A.C.). The catalysts were prepared by impregnating a commercially available activated carbon (Takeda Shirasagi C, wood made, 1400 m^2/g) with $Ni(OAc)_2$ from its aqueous solution(*1*). After drying in an air oven at 120°C for 24 h the catalysts were used without any further activation. The products were analyzed by an on-line GC (1-m Porapak N, 170°C). In order to keep the MeOH conversion below 10% and the by-product formation still detectable in the catalytic runs to determine reaction orders, the following reaction conditions were used: partial pressures CO, 0.428–4.12 atm; MeI, 0.056–0.407 atm; MeOH, 0.343–2.48 atm; MeOD, 0.772–2.48 atm; H_2, 0 or 0.1 atm; N_2, balance gas to 6 atm; 2.5 wt% Ni/A.C., 280°C, W/F = 0.25 g · h/mol. Under those conditions in the presence of H_2, the application of MeOD led to considerable deactivation. Therefore, its reaction orders were calculated from the relative rates. The latter were obtained from the stepwise activity changes after MeOD feed (partial pressure) changes.

Temperature-programmed reaction (TPR) measurements were carried out in H_2 flow without air contact of the used catalysts. X-ray diffraction (XRD) plots were recorded with a Rigaku Rotaflex instrument using Cu$K\alpha$ irradiation (40 kV, 100 mA). Exclusively Ni[0] peaks were observed for all used catalysts. GC–MS investigations were carried out with a Shimadzu QP-1000 (MS, 70 eV; GC, Gaskuropack 54). The XPS spectra were recorded with a Shimadzu ESCA-850 spectrometer using Mg$K\alpha$ radiation (10 kV, 30 mA). The binding energy scale was calibrated with NiO.

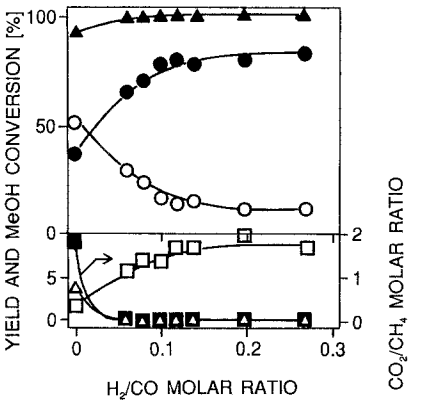

FIG. 1. Hydrogen effects on the yields of CH_3COOH (●), CH_3COOCH_3 (○), CH_3OCH_3 (△, CH_4 (□), CO_2 (■), and on the CH_3OH conversion (▲). Reaction conditions; 250°C, 11 atm, W/F = 5 g-cat · h/mol, CO/MeOH/MeI = 100/19/1.

RESULTS AND DISCUSSION

Promoting Effect of Hydrogen

Figure 1 illustrates the promoting effect of H_2 on the vapor-phase carbonylation of methanol. The carbonylation activity and the undesired CH_4 formation increase with the H_2/CO ratio. The same effect has been found at low methanol conversion levels (*5*). Mechanistic aspects of the promotion and the observed suppression of the CO_2 formation are discussed later. At high MeOH conversion levels, the increasing hydrogen partial pressure leads simultaneously to higher acetic acid (AcOH) and lower AcOMe yields (Fig. 1). This can be interpreted by the observation that, in the presence of water formed during the AcOMe formation, hy-

TABLE 1

Reaction Orders of CO, MeI, MeOH, and MeOD

Reactant	H_2 pressure (atm)	Reaction order[a] relative to formation of					
		AcOH + AcOMe		CH_4		DME	
CO	0	0.43	(0.04)	−0.26	(0.02)	−0.04	(0.05)
	0.1	0.69	(0.03)	−0.16	(0.05)	0.29	(0.07)
MeI	0	0.17	(0.09)	0.24	(0.12)	0.85	(0.08)
	0.1	0.65	(0.16)	0.08	(0.03)	1.13	(0.09)
MeOH	0	0.73	(0.03)	0.83	(0.05)	1.04	(0.03)
	0.1	0.71	(0.16)	0.79	(0.09)	1.13	(0.03)
MeOD	0	0.69	(0.09)	0.70	(0.08)	1.04	(0.07)
	0.1	0.81[b]	(0.05)	0.76[b]	(0.06)	1.17[b]	(0.07)

Note. Reaction conditions, partial pressures: CO, 0.428–4.12 atm; MeI, 0.056–0.407 atm; MeOH, 0.343–2.48 atm; MeOD, 0.772–2.48 atm; H_2, 0 or 0.1 atm; N_2, balance gas to 6 atm; 2.5 wt% Ni/A.C., 280°C, W/F = 0.25 g · h/mol.

[a] Standard deviations of the reaction orders in parentheses.

[b] From relative rates (see Experimental, obtained by MeOD feed rate changes during H_2-caused deactivation).

drogen also accelerates the carbonylation of AcOMe to AcOH (*3–5*). Corresponding to the suggestion that hydrogen induces an increased number of active Ni sites (*3*), which is limited by the Ni content of the catalyst, the product yields approach limits at higher H_2 partial pressures.

Hydrogen Influence on Reaction Orders

The reaction orders with regard to carbonylated products were already discussed (*1*), while those related to the by-products DME and CH_4 have not been published. Table 1 shows reaction orders of feed gas components. The relatively high reaction orders of CO and MeOH/MeOD indicate that the CO insertion and the reductive methanolysis are rate-determining steps. Because of the low reaction order, MeI is assumed not to participate in rate-determining steps even though its presence is crucial. Based on other findings, a rather complex mechanism including a number of possible pathways are discussed later. MeI and CO form the essential acyl–Ni–I species. Their reaction orders on acyl group formation were increased in the presence of hydrogen. Probably steps other than acyl species generation are promoted by hydrogen and the above-mentioned step in the catalytic cycle becomes more rate-determining. The high orders of MeOH and MeOD were not influenced by hydrogen, indicating an unchanged mechanism with regard to both reactants. This seems to contradict former results, but it should be noted that the reaction orders shown in Table 1 were determined under different conditions, as described in Ref. (*4*).

The CH_4 formation is suppressed by CO either in the absence or in the presence of hydrogen. Because of the small MeI reaction order on this side reaction, CH_4 might be formed at Me–Ni–I species, which are themselves quickly formed by addition of MeI to Ni[0] particles. As the high and non-H_2-influenced reaction orders show, MeOH and MeOD provide the hydrogen for the hydrogenolysis of the Me–Ni–I species, which can also afford acyl–Ni–I complexes via migrative CO insertion. The hypothesis that MeOH/MeOD and CO compete for the Me–Ni–I species explains the suppressed CH_4 formation with increasing CO partial pressure. The CO reaction order on the DME formation was increased in the pres-

ence of hydrogen. The reason for this effect is not yet clear. As the high reaction orders of MeOH/MeOD and MeI show, the DME formation is largely unaffected by H_2 and is generated from MeI and MeOH. The different reaction orders of MeI with respect to acyl compounds, CH_4 and DME formation suggests that DME generation does not necessarily proceed via Me–Ni–I species. Experiments with the unloaded carrier show that DME is also generated on activated carbon. On the other hand, studies on the effects of the Ni loading (see below) demonstrated that DME is also formed at active Ni sites.

Temperature Effects in the Presence of Hydrogen

Figure 2 shows the temperature dependence of main- and by-product formation related to Ni at low conversion levels (<13%). The higher carbonylation activity at higher temperatures in the absence of H_2 is already known (*1*). After introduction of H_2, at lower temperatures (220 and 250°C) the activity increased during a visible induction period to a constant level. At 280 and 300°C, the activity maximum was reached within a few minutes and was followed by a considerable activity decline. As shown by XPS investigations (*5*), the Ni(0)/Ni(II) ratio of 2.5 for a catalyst used in the absence of H_2 increased to 4.5 in its presence. Because other experiments (see below) demonstrated that H_2 does not reach the coordination spheres of active Ni particles, it can be concluded that the H_2 reduces inactive Ni[II] species such as $Ni(OAc)_2$, NiO, NiI_2, or Ni-methoxide to Ni[0] particles, thus providing more potentially active Ni for the catalytic cycle. With increasing temperatures, shorter induction periods for achieving the activity maxima were observed, which reflect increasing Ni[II]-reduction rates. It is noteworthy that the carbonylation activity changes (Fig. 2) were accompanied by those for the CH_4 and DME formation. In accordance with the low reaction order of MeI (Table 1), this suggests that CH_4 is at least generated at the Ni species involved in the carbonylation cycle. Used catalysts were studied by XRD after different process times (Table 2). No Ni peaks have been detected for catalysts used in the absence of H_2 (*4*) indicating small metal particle sizes. With progressive deactivation in the presence of H_2, enhanced Ni aggregation occurred. Obviously, larger Ni[0] crystallites have fewer active Ni sites available for the catalytic cycle, which requires Ni ensembles with three free coordination sites for the oxidative addition of MeI and the subsequent migrative CO insertion. Under the chosen conditions, the DME formation correlated to the formation of acyl compounds, suggesting that it was partly generated via Ni catalysis.

Effects of Ni Loading

The catalytic runs were started with the unreduced $Ni(OAc)_2$/A.C. catalysts. According to the mechanism of the carbonylation reaction, all the feed gas components CO, MeOH, and MeI are involved in the active center formation. Thereby, the catalyst with the lowest loading of 0.2 wt% Ni exhibited the longest induction period (Fig. 3), which is explained by the highest W_{cat}/F for this catalyst to keep W_{Ni}/F constant. The steady-state conditions including adsorption/desorption equilibria might be reached later because of the high specific surface area of the porous carrier (about 1200 m^2/g), where the reactants must be adsorbed and subsequently transported to supported Ni particles.

Provided that the catalytic cycle proceeds at small Ni clusters capable of sintering under H_2 influence, lower Ni loadings ought to slow the Ni aggregation causing the deactivation. Indeed, in the presence of hydrogen, catalysts with lower Ni loadings (0.2 and 0.5 wt%) showed the lowest deactivation rate (Fig. 3). As shown in Fig. 4, the deactivated catalyst recovered its activity after stopping the H_2 flow. The reactivation most likely

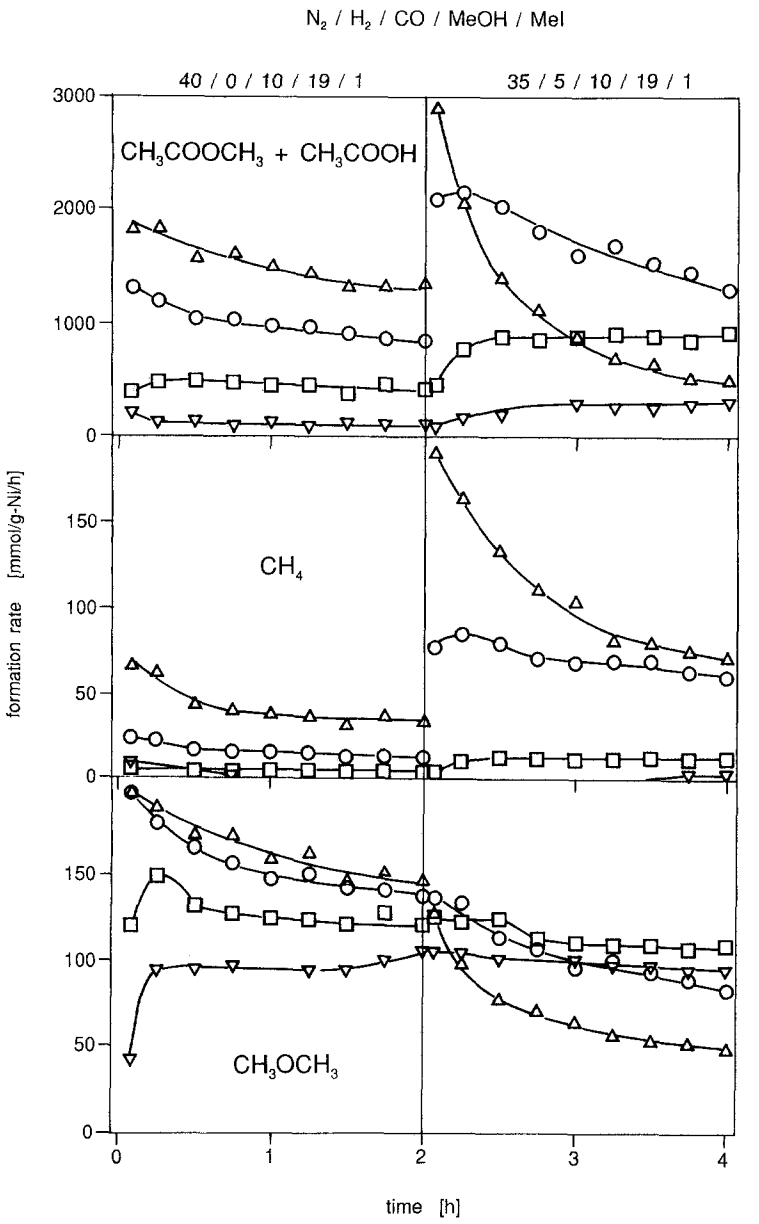

FIG. 2. Temperature dependence of hydrogen effects, W/F = 0.25 g-cat · h/mol, 6 atm, 2.5 wt% Ni/A.C., 220°C (▽), 250°C (□), 280°C (○), 300°C (△).

proceeds via CO attack at the Ni[0] crystallites, thus affording Ni carbonyls that redisperse the metal over the catalyst surface.

The relative activity change ($r_{max}(H_2)/r_0$), which is defined as the quotient of maximum rate in the presence of H_2 and the rate before H_2 introduction, is larger at higher loadings for the CH_4 and the acyl compound formation (Fig. 5). This suggests that at low loadings the Ni is already highly dispersed. In that case the dispersion cannot increase as strongly as in the case of higher loaded cata-

TABLE 2

H_2 Effects on Catalytic Activity and Ni Particle Size

Sample no.	Time on stream (min)	Formation rate of		Average Ni[0] particle size[a] (nm)
		AcOH + AcOMe (mmol/gNi/h)	CH_4	
1	180	1320	35	No Ni peak detected
2	5	1960	230	22
3	30	1100	140	34
4	60	800	140	31
5	120	510	70	92

Note. Reaction conditions: 2.5 wt% Ni/A.C., 300°C, 6 atm, W/F = 0.25 g-cat · h/mol; sample 1, $N_2/H_2/CO/MeOH/MeI$ = 40/0/10/91/1; samples 2–5, $N_2/H_2/CO/MeOH/MeI$ = 35/5/10/19/1.

[a] Calculated from peak broadening in the XRD spectra.

lysts. Furthermore, the curves in Fig. 5 reveal that with increasing Ni loadings, the CH_4 formation is promoted more strongly than the carbonylation. This is explained by the following hypothesis. The CH_4 formation demands active centers with at least two unsaturated coordination sites (^2M or ^3M sites) to form the Me–Ni–I precursors. The carbonylation can only take place at centers with three free coordination sites (^3M sites) because this reaction requires additionally the migrative CO insertion to form acyl–Ni–I species from the Me–Ni–I species. Related to their mass, larger Ni particles contain fewer ^2M sites located on edges or steps and even fewer ^3M sites represented by corner or kink atoms. If the CO-induced dispersion results in larger Ni particles at higher loadings, the number of ^2M sites will increase relative to that of ^3M sites and the promotion of the reaction path with smaller steric requirements, which is the CH_4 formation, should be stronger.

The selectivity dependence on the metal loading in the presence of H_2 is presented in Fig. 6. Although the MeOH conversion was quite similar, at lower Ni contents significantly higher methane and AcOH selectivities were obtained. The higher AcOH selectivity at low loadings can be explained by increased H_2O formation from DME (related to Ni; see Fig. 3). H_2O can attack Ac–Ni–I species or hydrolyze AcOMe to form AcOH. The latter reaction is less probable at the applied low conversion levels.

Activity declines at 250°C in the presence of H_2 and at low MeI partial pressure are already known (*4b*). Thus, catalyst samples at the activity maxima and those after the deactivation (Fig. 7) were investigated by XRD. At the activity maxima, no Ni peak was detected by XRD. After the deactivation, caused by a low MeI pressure, an average Ni[0] particle size of 100 nm was obtained for a catalyst loaded with 2.5% Ni. The reason for this deactivation is discussed in the next section. However, low Ni loadings can be expected to slow the H_2-induced deactivation by aggregation. This has been verified for a 0.5 wt% Ni catalyst, even though the total activity loss is not yet clear (Fig. 7).

Hydrogen Effects at Various MeI Partial Pressures

The increase in the reaction order of MeI indicates the increasing importance of the promoter in the presence of H_2 (Table 1). Experiments with different MeI partial pressures (*4b*) indicate that if the promoter concentration is too low then deactivation can also occur. This is in accordance with the as-

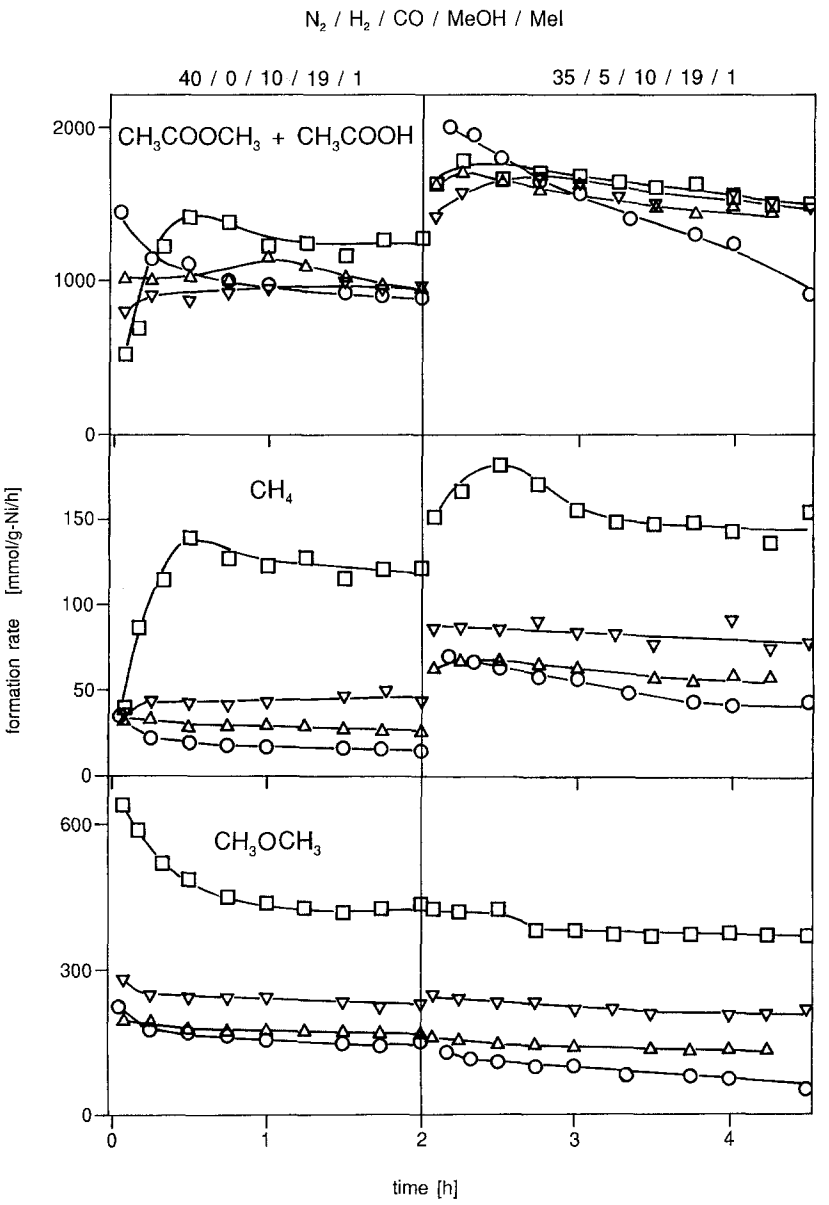

FIG. 3. Hydrogen effects on catalysts loaded with 0.2% (□), 0.5% (▽), 1.0% (△), and 2.5% (○) Ni/A.C., 280°C, W/F = 6.25 mg-Ni · h/mol, 6 atm.

sumption that the deactivation results from sintering of small Ni[0] particles. It is apparent that MeI prevents these active Ni particles from sintering by the formation of Me–Ni–I species. If the last-mentioned step is restrained by a too low promoter partial pressure, the deactivating aggregation of small Ni[0] species proceeds faster than their conversion to active sites such as Me–Ni–I or acyl–Ni–I species. As indicated in Fig. 7, at higher MeI pressures the H_2-induced promotion of the reaction remains at a high level.

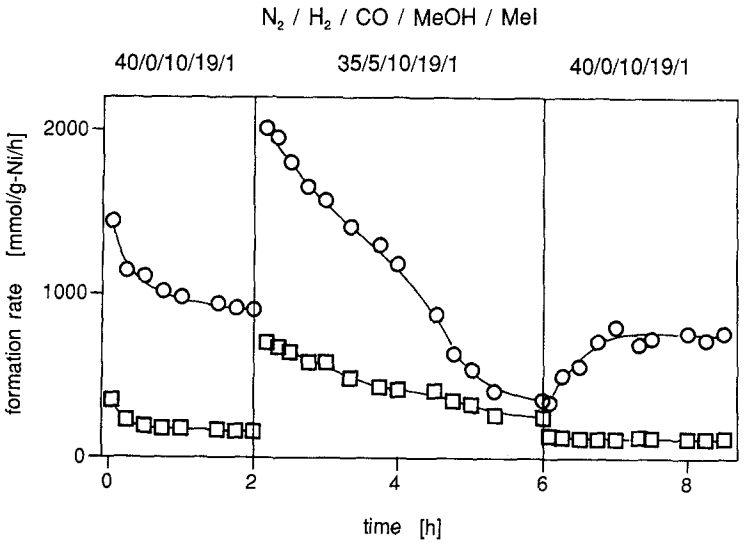

FIG. 4. Catalyst reactivation after hydrogen-induced deactivation, 10-CH_4 (□), CH_3COOCH_3 (○); reaction conditions as in Fig. 3.

TPR Investigations

TPR provides valuable information on the Ni dispersity of used catalysts. With regard to the CO and CO_2 release, the spectra recorded for catalysts used at different H_2 partial pressures were rather similar. In Fig. 8, carbonylation and CH_4 formation activities at different H_2 partial pressures are compared with the CH_4 TPR plots of the used catalysts. Since Ni on activated carbon does not catalyze the hydrogenation of chemisorbed CO to CH_4 (6), the latter can only be formed from acetate species or acyl–Ni–I or Me–Ni–I species. A comparison between the curves for CO, CO_2, and the dominant CH_4 makes clear that the CH_4 release, especially above 400°C, is mainly generated from Me–Ni–I species, which are unable to form CO or CO_2. The correlation between reac-

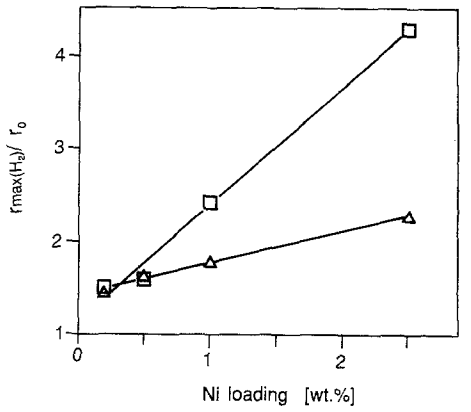

FIG. 5. Hydrogen-induced relative acceleration of carbonyl compound (△) and methane (□) formation (see text) dependent on the Ni loading; reaction conditions as in Fig. 3.

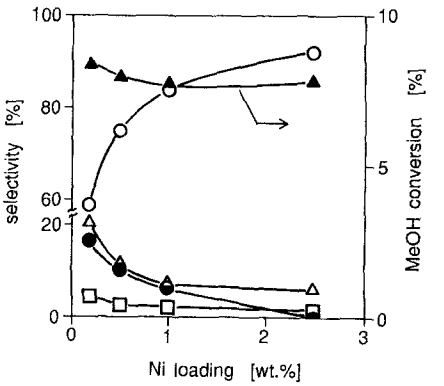

FIG. 6. Selectivities of CH_3COOCH_3 (○), CH_3COOH (●), CH_3OCH_3 (△), and CH_4 (□) and CH_3OH conversion (▲) at various Ni loadings after 1 h H_2 influence; reaction conditions as in Fig. 3.

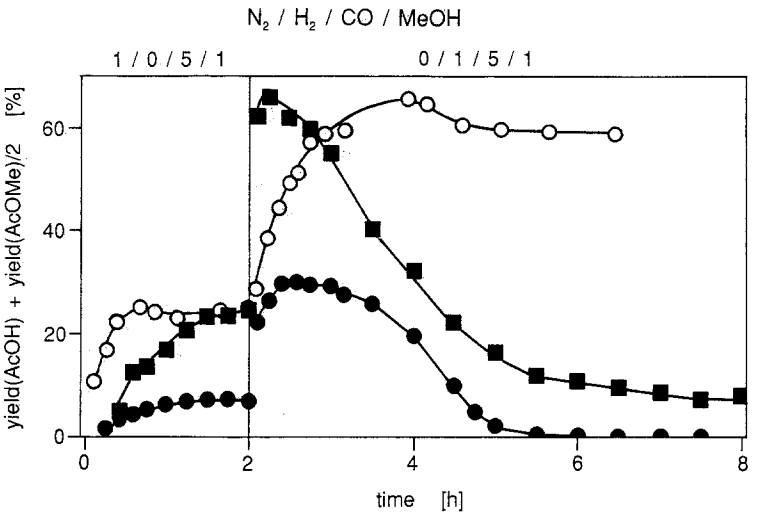

FIG. 7. Hydrogen-induced activity changes with process time at low MeI partial pressures for 0.5% Ni/A.C., MeOH/MeI = 99 (●), 2.5% Ni/A.C., MeOH/MeI = 99 (■), and 2.5% Ni/A.C., MeOH/MeI = 50 (○), 250°C, W/F = 2 g-cat · h/mol, 11 atm.

tivities and released amounts of CH_4 above 400°C proves that the H_2-caused acceleration of the reaction is brought about by an increase in the number Me–Ni–I species.

Deuterium Effects

While the promoting effect of deuterium on the carbonylation reaction was comparable to that of H_2, only a few deuterated products were found (Table 3) (*4*). These findings disclose H_2 interactions with active Ni complexes and, in particular, CH_4 formation by hydrogenolysis from acyl- or methyl-Ni intermediates. Inspired by the observed reaction orders of MeOH on the CH_4 formation, we studied the carbonylation of MeOD at

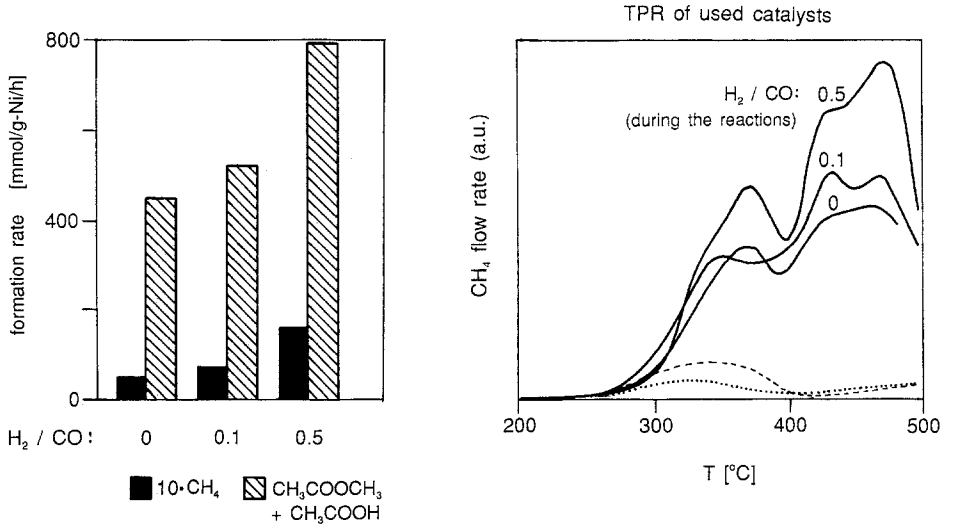

FIG. 8. Reactivity increased by H_2 and TPR of the used catalysts, (———) CH_4, (– – –) CO, (· · ·) CO_2; reaction conditions: 250°C, W/F = 0.75 g-cat · h/mol, 6 atm.

TABLE 3

Deuterium Content in Reaction Products

	Product yield [%]					
	CH_4	AcOMe	AcOH	DME		
Without H_2	1.3	45.7	8.9	6.5		
With H_2	5.4	10.0	84.6	0		
With D_2	5.0	4.1	91.0	0		
Fragment	CH_4	CH_3CO	OCH_3	CH_3CO	OH	H_2O
D content (%)	3.6	1.2	0.0	3.0	0.0	0.0

Note. 2.5 wt% Ni/A.C., 250°C, 11 atm, W/F = 5 g · h/mol, CO/MeOH/MeI/D_2(H_2) = 43/9/1/11.

280°C to clarify the open question concerning the hydrogen source for methane formation from Me–Ni–I species. During the catalytic runs for the determination of reaction orders, it has been observed that MeOD affords distinctly smaller methane yields than MeOH (ca. 50–70% related to MeOH; see also Table 4, runs 1,2 and 4,5, respectively). This deuterium effect was a first hint of the methanol hydroxyl group behaving as a H/D donor. Thus, only CH_3D was detected by GC–MS at MeOD conversion levels of ca. 5 and 70%, respectively. Consistent with the observed D_2 effects (*4*), even in the presence of H_2, which markedly increased the methane formation (Table 4, run 2,3), only CH_3D was observed. Since MeOD decomposition to syngas would lead to a D/H ratio of 1/3 and would imply a CH_3D/CH_4 ratio of 1/3, which has not been confirmed, this process can be excluded with respect to the CH_4 formation. The probable mechanism for the methane formation is discussed in the next section.

Mechanistic Considerations

On the basis of the previous results (*3–6*) and the findings of this work, a rather complex mechanism for the vapor-phase carbonylation of MeOH is proposed (Scheme 1). This mechanism does not consider the manner of adsorption of the gaseous reactants on the catalyst. The size and nature of the active species **1–4** supported on the

TABLE 4

Deuterium Effects on the Vapor-Phase Carbonylation of Methanol

Run	1[a]	2[a]	3[a]	4[b]	5[b]
$N_2/H_2/CO/MeOH/MeI$	40/0/10/19/1			0/0/20/19/1	
$N_2/H_2/CO/MeOD/MeI$		40/0/10/19/1	39/1/10/19/1		0/0/20/19/1
Yield (%) CH4	0.04	—	—	1.7	—
CH_3D	—	0.02	0.06	—	1.1
CH_3OCH_3	0.65	0.55	0.32	9.2	8.2
CH_3COOCH_3	4.2	4.6	5.6	47.0	44.2
CH_3COOH	0.0	—	—	8.7	—
CH_3COOD	—	0.0	0.0	—	12.7

Note. Reaction conditions: 2.5 wt% Ni/A.C., 280°C.
[a] 6 atm, W/F = 0.25 g-cat · h/mol.
[b] 11 atm, W/F = 3 g-cat · h/mol.

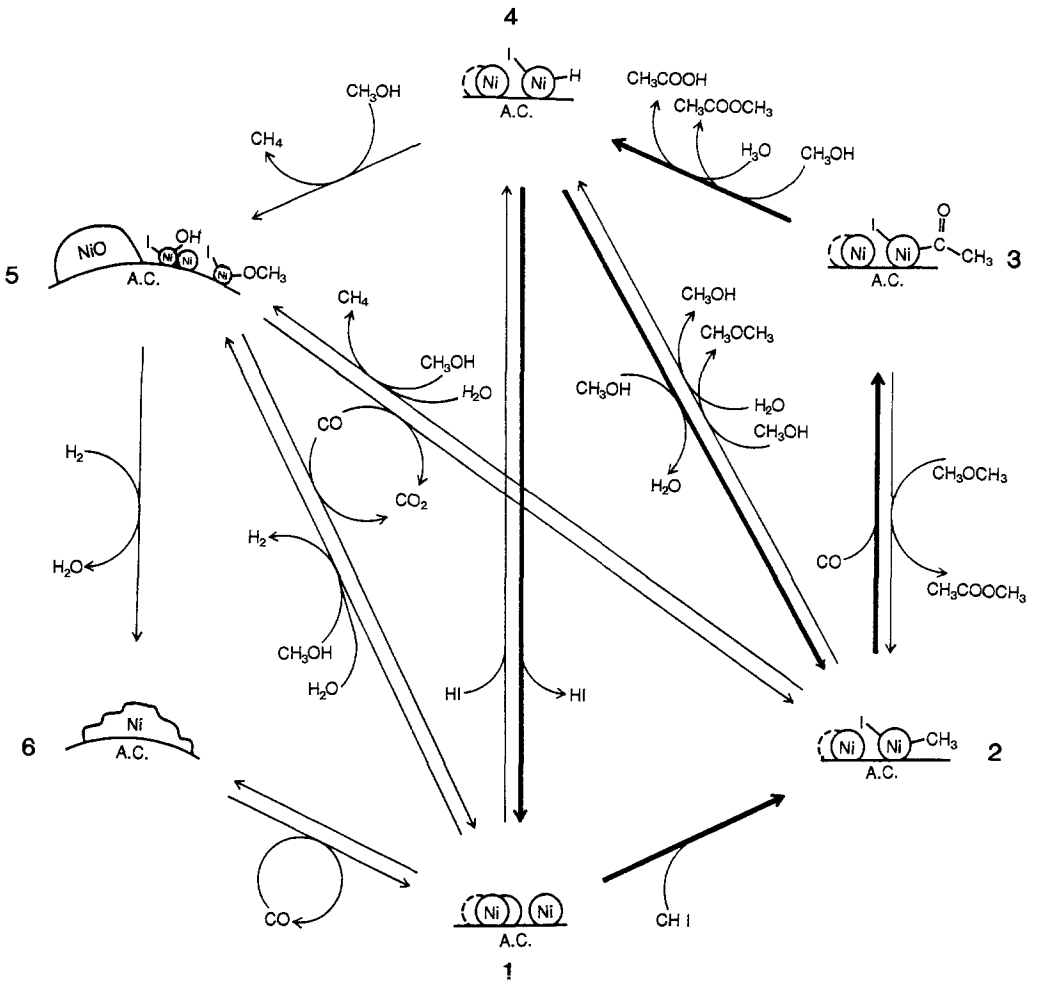

SCHEME 1. Mechanism for the Ni-catalyzed vapor-phase carbonylation of methanol.

carbon are not yet clarified. The carbonylation could occur at small Ni clusters as well as at one-atomic Ni complexes coordinated to the aromatic systems of the active carbon carrier. The main routes of the carbonylation are identified in Scheme 1 by bold arrows. A sequence of oxidative MeI addition, migrative CO insertion, and reductive methanolysis (species **1–4**) affords AcOMe and AcOH. Figure 9a illustrates the nucleophilic attack of MeOH on the carbonyl group of the acyl species to form AcOMe. Water resulting from the generation of AcOMe and dimethyl ether may react analogously with species **3** to AcOH. Independent of this, at longer contact times and higher conversions, AcOMe is converted to AcOH (*3–5*). The transformation of H–Ni–I to the important Me–Ni–I species should also occur via nucleophilic substitution by MeOH. This implies that the catalytic cycle does not exclusively proceed via free Ni[0] species, which is consistent with the fact that small amounts of oxygen in the feed gas do not act as a catalyst poison (*7*).

The promotion effect of hydrogen can be attributed to its attack on NiO particles (**5**), thus leaving smaller or larger Ni[0] particles that are more easily attacked by CO than Ni[II]. After the reduction of the Ni[II] pre-

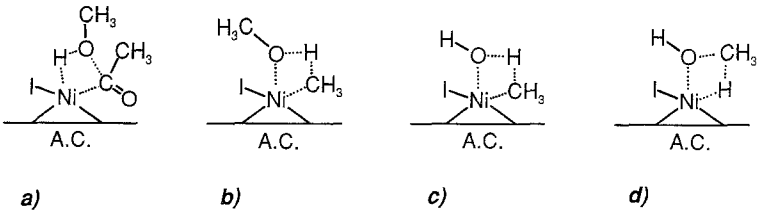

FIG. 9. Possible transition states for the formation of CH_3COOCH_3 (a) and CH_4 (b, c, d). It is not yet clear whether the formations really proceed via concerted mechanisms.

cursors, hydrogen does not react with species **2,3,** and **4**. Supported Ni[0] particles are supposed to react with CO to form subcarbonyls or $Ni(CO)_4$. Their surface- or gas-phase- diffusion probably affects an active metal dispersion on the catalyst surface. MeI, HI, CO, H_2O, and MeOH keep small Ni[0] particles (species 1) in the catalytic cycle (species **1–5**). Higher temperatures render their chemisorption more difficult and allow the aggregation of species **1**. The same is the case for low MeI or CO partial pressures. The mechanism of the Ni sintering during the carbonylation is not yet clarified.

Hypothetical CH_4 formation transition states are supposed to result from species **2** and **4** (Figs. 9b–9d). The role of methanol in the reactions of species **2** and **4** is rather complex. However, the methane formation requires the conversion of methanol. On the other hand, species **2** reacts with CO to form the acyl species **3**. The high reaction order of methanol with respect to the CH_4 formation and the suppression of this reaction by CO (Table 1) is consistent with the proposed mechanism.

The CO-induced reduction of the resulting NiO, NiOH, or NiOMe species explains the occurrence of CO_2 even after the induction period. The proposed mechanism is also consistent with the suppressed CO_2 formation in the presence of H_2 (*4*). As the stronger reducing agent, H_2 takes over this reduction, thus suppressing the competitive reduction by CO affording CO_2.

Although DME is produced on the support, its formation is also catalyzed by Ni, most probably via Me–Ni–I species **2**. The DME carbonylation should proceed via nucleophilic attack on acyl species **3**. This does not require a previous cleavage by HI to MeI and MeOH and is supported by the fact that DME can be carbonylated in water- and HI-free media (*8*).

CONCLUSIONS

In the Ni-catalyzed vapor-phase methanol carbonylation, hydrogen can act as a promoter as well as an inhibitor. While the promotion of the carbonylation reaction occurs due to an increase in the number of active Ni centers, the observed deactivation has been shown to result from Ni aggregation.

The catalytic reaction as well as the undesired methane formation occurs at small Ni species whose structure is not yet clear. Because methane is formed from MeI and MeOH via Me–Ni–I species, its formation will always accompany the main reaction; however, it can be regulated by the CO partial pressure and other reaction conditions.

ACKNOWLEDGMENTS

Thanks are given to the Japanese Ministry of Education, Science and Culture (MONBUSHO) for a scholarship for S.B. and to the Toyo Engineering Corp. (Japan) for financial support.

REFERENCES

1. Fujimoto, K., Shikada, T., Omata, K., and Tominaga, H., *Ind. Eng. Chem. Prod. Res. Dev.* **21,** 429 (1982).
2. Ritzkalla, N., *in* "Industrial Chemicals via C_1 Processes" (D. R. Fahey, Ed.), Vol. 328, p. 61. Am. Chem. Soc. Symp. Ser., Washington, DC, 1987.
3. Fujimoto, K., Mazaki, H., Omata, K., and Tominaga, H., *Chem. Lett.,* 895 (1987).

4. (a) Omata, K., Fujimoto, K., Yagita, H., Mazaki, H., and Tominaga, H., *in* "Studies in Surface Science and Catalysis" (B. Delmon and J. T. Yates, Eds.), Vol. 36, p. 245. Elsevier, Amsterdam/Oxford/New York/Tokyo, 1988. (b) Fujimoto, K., Mazaki, H., Omata, K., Yagita, H., Kikuchi, K., and Tominaga, H., *in* "Proceedings, 9th International Congress on Catalysis, Calgary, 1988" (M. J. Phillips and M. Ternan, Eds.), Vol. 3, p. 1051. Chem. Institute of Canada, Ottawa, 1988.
5. Omata, K., Fujimoto, K., Yagita, H., Mazaki, H., and Tominaga, H., *Mater. Res. Soc. Int. Meeting Adv. Mater.* **2,** 355 (1989).
6. Omata, K., Fujimoto, K., Shikada, T., and Tominaga, H., *Ind. Eng. Chem. Res.* **27,** 2211 (1988).
7. Omata, K., *et al.*, unpublished data.
8. Shikada, T., Fujimoto, K., Miyauchi, M., and Tominaga, H., *Appl. Catal.* **7,** 361 (1983).